Ordered Structures of Block Polymer/Homopolymer Mixtures. 3. Temperature Dependence

Hideaki Tanaka† and Takeji Hashimoto*

Department of Polymer Chemistry, Faculty of Engineering, Kyoto University, Kyoto 606, Japan

Received December 27, 1990; Revised Manuscript Received May 24, 1991

ABSTRACT: The ordered structures in the binary mixtures of poly(styrene-*block*-isoprene) (SI) and polystyrene (HS) were investigated as a function of temperature T using small-angle X-ray scattering. The mixtures were studied in a regime in which HS is solubilized in polystyrene microdomains of SI, as a function of the volume fraction, ϕ_{HS}, and the molecular weight, M_{HS}, of HS as well as the total polymer volume fraction ϕ_p ($0.66 \leq \phi_p \leq 1$) when dioctyl phthalate (DOP) was added to the mixtures as a neutral solvent. The exponent n characterizing the temperature dependence of the interdomain distance ($D \sim T^{-n}$) was found to depend strongly on ϕ_{HS} and M_{HS}, n increasing with increasing ϕ_{HS} and decreasing M_{HS}. Such a scaling behavior as $(D - D_S)/D_S \sim \epsilon_T = (\chi_{eff} - \chi_{ODT})/\chi_{ODT}$ was found under the condition that $\chi_{eff} = A + B\phi_p^{2/3}/T$. Here D_S is the wavelength of the dominant mode of the composition fluctuations in the disordered state, χ_{eff} is the effective Flory interaction parameter between polystyrene and polyisoprene per segment base in presence of DOP when DOP is added to the mixture, and χ_{ODT} is χ_{eff} at the order–disorder transition temperature.

I. Introduction

In our previous papers of this series,[1,2] we reported the effects of solubilization of homopolystyrene (HS) on the ordered microdomains of a poly(styrene-*block*-polyisoprene) (SI) diblock polymer. The solubilization of HS into polystyrene (PS) microdomains and the resulting changes of the microdomain morphology and size were systematically investigated as a function of the molecular weight (M_{HS}) and the volume fraction of HS (ϕ_{HS}) for the solvent-cast films.

Here we extend the study to investigate the morphology and size of the ordered microdomains as a function of temperature, T. For example, the interdomain distance, D, is studied quantitatively and systematically as a function of T, ϕ_{HS}, M_{HS}, and ϕ_p as well, where ϕ_p is the total volume fraction of the polymers ($0.66 \leq \phi_p \leq 1$) when dioctyl phthalate (DOP) was added to the mixtures as a neutral solvent. The values $D(T;\phi_{HS},M_{HS},\phi_p)$ assessed by the small-angle X-ray scattering (SAXS) method, again in a regime in which all HS homopolymers are solubilized into the PS microdomains, will be analyzed in terms of the Flory interaction parameter χ_{eff} between PS and polyisoprene (PI) block polymers per segment base, which was determined also as a function of T, M_{HS}, ϕ_{HS}, and ϕ_p from the SAXS analyses in the disordered state.[3]

It is worth noting here that there are some earlier interesting experimental reports[4–6] on the temperature dependence of the ordered microdomains and the order–disorder transition for binary mixtures of block polymers and the corresponding homopolymers. However, the temperature change of the ordered microdomains has never been analyzed as a function of ϕ_{HS}, M_{HS}, and ϕ_p so systematically as we intended to investigate here.

II. Experimental Methods

Table I summarizes characteristics of the samples used in this work, which are identical with those used in previous papers.[1–3] The method of preparing as-cast films with or without DOP is also the same as that used in previous work.[1–3] The morphology of the microdomains at various temperatures was investigated in situ by the SAXS method as previously reported.[7–9] The microdomains are usually oriented to some extent in the as-cast films. The orientation is randomized at 50–80 °C, and the SAXS patterns are confirmed to be circularly symmetric about the incident beam spot by using a point-focused X-ray beam. This is to facilitate the desmearing of the SAXS profiles measured by the line-focused X-ray beam with a rather narrow slit height[8] for quantitative estimations of $D(T;\phi_{HS},M_{HS},\phi_p)$. The SAXS profiles were corrected for absorption, air scattering, the thermal diffuse scattering, and slit-height and -width smearings as reported previously,[8,9] unless otherwise stated.

Table I
Characteristics of Polymers Used in This Study

specimen	$M_n \times 10^{-3}$ [a]	S/I (wt %/wt %)	M_w/M_n [c]
SI	31.6	48/52[b]	1.07
S17	16.7	100/0	1.02
S10	10.2	100/0	1.02
S04	4.4	100/0	1.06
S02	2.3	100/0	1.10

[a] Determined by membrane osmometry or vapor pressure osmometry. [b] Determined by elemental analysis. [c] Determined by size-exclusion chromatography.

III. Results and Discussion

1. SAXS Profiles as a Function of Temperature. All the SAXS profiles shown in this section are left intentionally smeared, because the first-order scattering maxima for some profiles, especially those for lamellar microdomains, are too sharp for the conventional desmearing procedures to be applicable. However, all other corrections are made. Moreover, the value D was determined from the peak positions of the desmeared profiles.

Figure 1 shows the SAXS profiles for the pure SI block polymer at various temperatures. Up to about 120 °C, the first-, third- and fifth-order maxima are discernible, implying the existence of the alternating lamellar microdomain with a long-range spatial order. The second- and fourth-order maxima are suppressed due to the fact[2] that the volume fraction of one type of lamella is close to 0.5. Even at higher temperatures up to 180 °C, the first- and third-order maxima exist, although their peak intensities and positions systematically decrease and shift toward larger scattering vector $q = (4\pi/\lambda)\sin\theta$, respectively, where λ and 2θ are the wavelength of the X-ray and the scattering angle, respectively. Thus the ordered lamellar microdomains persist up to 180 °C for SI.

† Present address: Mitsubishi Kasei Corp., Research Center, 1000 Kamoshida-cho, Midori-ku, Yokohama 227, Japan.

0024-9297/91/2224-5713$02.50/0

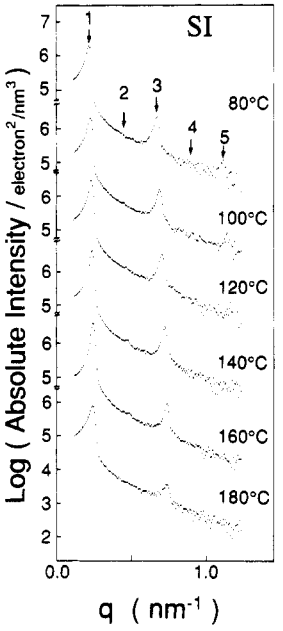

Figure 1. Smeared SAXS profiles for pure SI block copolymers measured in situ at 80–180 °C.

Figure 2 shows some representative SAXS profiles for the binary mixtures of SI and HS (S02) with the compositions of 80/20 (part a), 50/50 (part b), and 20/80 (part c) at various temperatures. We designate hereafter the binary mixture of SI and S02 with the respective compositions of 80 and 20 in weight percent as SI/S02 (80/20). This weight fraction of HS (W_{HS}) was converted to ϕ_{HS} for further analysis. Of course $\phi_{HS} \cong W_{HS}$. The mixture SI/S02 (80/20) (Figure 2a) shows the higher order peaks at the values q that are integer multiples of that (q_{m1}) for the first-order peak. Up to the fourth-order peaks, the third-order peaks are discernible at $T \leq 60$ °C and 60 $< T \leq 220$ °C, respectively, indicating existence of the lamellar microdomains at $T \leq 220$ °C. The mixture SI/S02 (50/50) (Figure 2b) shows the higher order peaks at the values q/q_{m1} of $1{:}\sqrt{3}{:}\sqrt{7}{:}\sqrt{9}$ at $T \leq 100$ °C. The peaks at $\sqrt{3}$ and $\sqrt{4}$ are presumably overlapped. The fourth-order peak at $q/q_{m1} = \sqrt{9}$ disappears at $T > 120$ °C, but up to the third-order peaks exist at least up to 160 °C, implying the existence of the hexagonally packed cylinders at $T \leq 160$ °C. The mixture SI/S02 (65/35) showed also the hexagonally packed cylinders up to 160 °C, though not shown here. The fourth-order peak existed up to a slightly higher temperature, i.e., 120 °C, than the case of SI/S02 (50/50). The mixture SI/S02 (20/80) (Figure 2c) shows the first- and second-order peaks at $q/q_{m1} = 1$ and $\sqrt{2}$ as marked by thin arrows, due to the interparticle interference of the spherical microdomains. It also shows the broad first- and second-order peaks, as marked by thick arrows, due to the intraparticle interference of the single spherical microdomain at q's satisfying $q\bar{R} = 5.765$ and 9.10 where $\bar{R}$ is the average radius of the spheres. The peaks at $q/q_{m1} = 1$ and $\sqrt{2}$ exist up to 160 °C. The second-order intraparticle peak disappears at $T \geq 100$ °C, but the corresponding first-order peak persists up to a higher temperature, i.e., up to $T \cong 140$ °C. Thus the spherical microdomains should exist at least up to 140 °C. The same conclusion was obtained for SI/S02 (35/65), though their SAXS profiles are not shown here.

Figure 3 shows some representative SAXS profiles for the mixtures of SI/S04 with the composition of 80/20 (part a) and 50/50 (part b), while Figures 4 and 5, respectively, show those for the mixtures of SI/S10 (80/20) (Figure 4a), SI/S10 (50/50) (Figure 4b), SI/S17 (80/20) (Figure 5a), and SI/S17 (50/50) (Figure 5b). All the mixtures with the 80/20 composition show the lamellar microdomain structure for all experimental temperatures, regardless of M_{HS} (cf. Figures 3a, 4a, and 5a). The temperature dependences of their SAXS profiles are qualitatively similar in that the peak shifts toward large q with raising temperature and the fifth-order peak is suppressed due to the PI lamella having a volume fraction close to 40%. Note that the nth-order peak tends to disappear when $n\phi$ becomes an integer (ϕ being the volume fraction of one type of domain), because the particle factor of the domain tends to go to zero at the nth-order peak position under this condition. However, there are some quantitative differences as to the peak shift with temperature

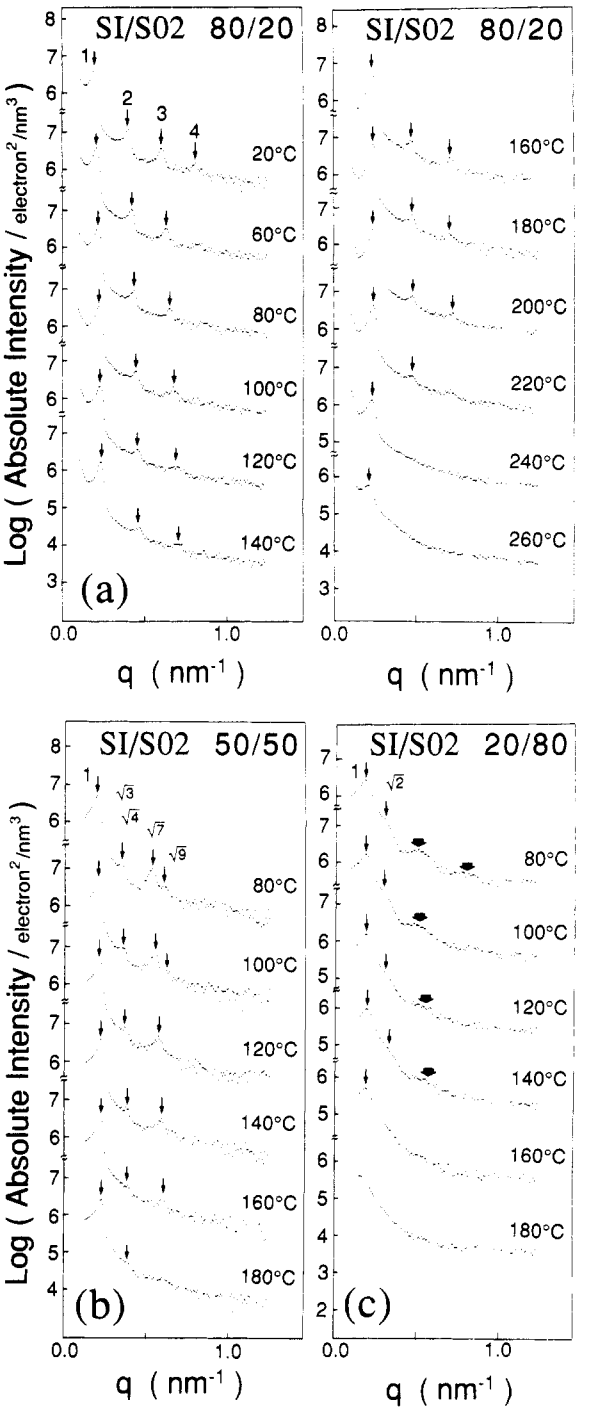

Figure 2. Smeared SAXS profiles for SI/S02 mixtures with compositions of (a) 80/20, (b) 50/50, and (c) 20/80 measured in situ at various temperatures.

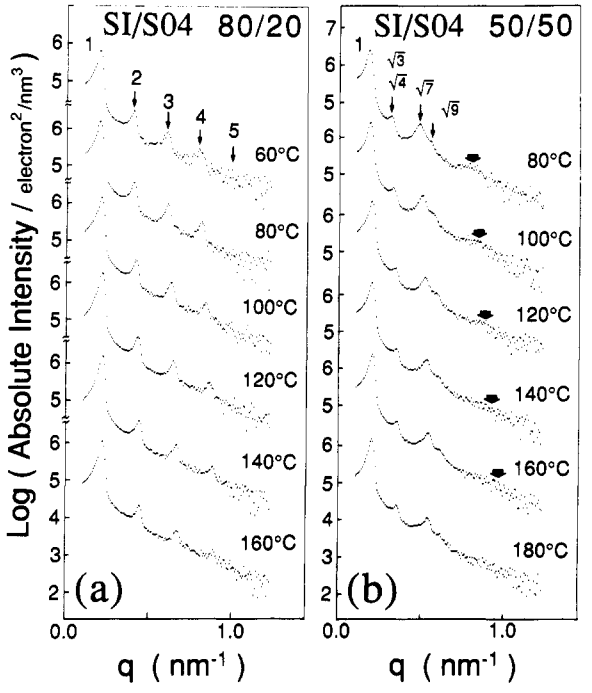

Figure 3. Smeared SAXS profiles for SI/S04 with compositions of (a) 80/20 and (b) 50/50 measured in situ at various temperatures.

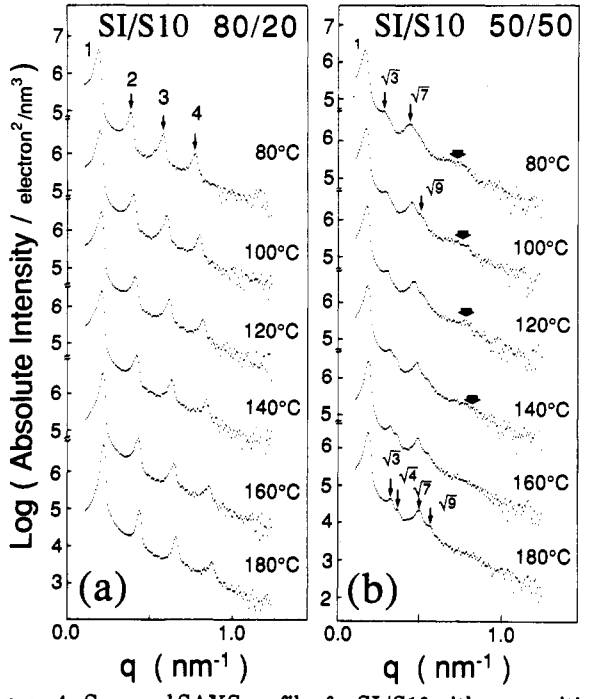

Figure 4. Smeared SAXS profiles for SI/S10 with compositions of (a) 80/20 and (b) 50/50 measured in situ at various temperatures.

and the stability of the higher order peak at higher temperatures.

The 50/50 mixtures of SI/S04 and SI/S10 show the cylindrical domain structure at all the temperatures covered in this experiment. The profiles show the peaks, as marked by thin arrows, due to the hexagonal lattice at the relative peak positions of 1, $\sqrt{3}$, $\sqrt{4}$, $\sqrt{7}$, and $\sqrt{9}$ up to 180 °C, and the broad second-order maximum, as marked by thick arrows, due to the single cylinder up to 160 °C. The peaks at $\sqrt{3}$ and $\sqrt{4}$ for the SI/S04 (50/50) are overlapped at all temperatures, while those for the SI/S10 (50/50) are overlapped at lower temperatures but split at higher temperatures (e.g., $140 \leq T \leq 180$ °C). The splitting reflects further ordering of the hexagonal packing

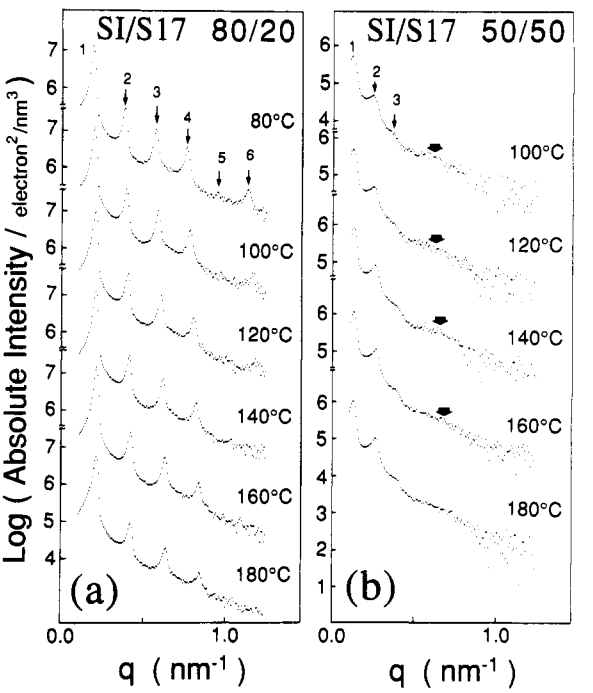

Figure 5. Smeared SAXS profiles for SI/S17 with compositions of (a) 80/20 and (b) 50/50 measured in situ at various temperatures.

due to thermal motions. The SAXS profiles for the 50/50 mixtures for SI/S17 (Figure 5b) are distinctly different from those for SI/S04 (Figure 3b) and SI/S10 (Figure 4b). They have three scattering maxima at the peak positions satisfying $q_m/q_{m1} = 1$–3 (marked by thin arrows) at all the tempertures and a broad maximum (marked by a thick arrow) up to 160 °C, suggesting the existence of lamellar microdomains rather than cylindrical microdomains. The broad maximum is due to the first-order maximum from the single PI lamella as previously found and quantitatively analyzed.[2,10]

The change of morphology from cylindrical to lamellar with increasing M_{HS} is due to the fact that the spatial distribution of the PS homopolymers solubilized in the PS microdomains depends on M_{HS}, as previously discussed.[2] The low molecular weight homopolymers tend to be solubilized uniformly in the domains ("*uniform solubilization*"), but the high molecular weight homopolymers tend to be solubilized in the middle of the domains ("*localized solubilization*"). In the case of uniform solubilization, HS swells PS domains both parallel (laterally) and normal to the interface (longitudinally). The lateral swelling causes some changes in the conformation of PI chains and hence in the curvature of the interface, giving rise to a driving force for morphological change.[2] On the other hand, in the localized solubilization, HS swells the PS domains only longitudinally but not laterally, which induces little change in the PI chain conformation and hence no morphological change.[2]

2. Order–Disorder Transition. The order–disorder transition (ODT) for the pure SI and the binary mixtures of SI/HS occurs at high temperatures[11,12] where the thermal degradation becomes significant. Dioctyl phthalate (DOP) was added to the systems as a neutral solvent to lower the ODT temperatures and to circumvent the difficulties associated with thermal degradation. The ODT temperatures T_b' (K) determined with DOP were then converted to those in bulk T_b (K) assuming the relationship

$$\phi_p/T_b' = 1/T_b$$

where ϕ_p is the total volume fraction of the polymer in the systems with DOP. It should be noted that this deter-

Table II
Order-Disorder Transition Temperatures (T_b') for a DOP Solution and (T_b) for Bulk

sample codes	composition, wt %/wt %	vol fraction of polym, ϕ_p	T_b', K	T_b,[a] K
SI		0.66	428	650
SI/S02	80/20	0.74	411	563
	65/35	0.75	381	516
	50/50	0.85	428	503
	35/65	0.85	425	500
	20/80	0.85	398	468
SI/S04	80/20	0.66	397	602
	50/50	0.66	392	606
SI/S10	80/20	0.66	407	615
	50/50	0.66	406	617
SI/S17	80/20	0.66	410	621
	50/50	0.66	431	653

[a] Determined from T_b' by assuming $\phi_p/T_b' = 1/T_b$.

Table III
Slope n on the Plot of log D vs log $(1/T)$

sample codes	composition, wt %/wt %	n for bulk	n for DOP solution
SI		0.333	0.333
SI/S02	80/20	0.500	0.468
	65/35	0.518	0.518
	50/50	0.689	0.659
	35/65	0.742	0.790
	20/80	0.825	0.906
SI/S04	80/20	0.458	0.408
	50/50	0.601	0.605
SI/S10	80/20	0.527	0.420
	50/50	0.520	0.417
SI/S17	80/20	0.437	0.450
	50/50	0.409	

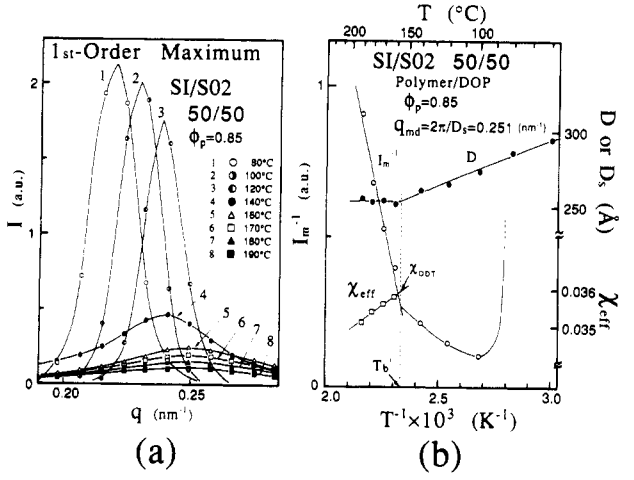

Figure 6. (a) Change of the desmeared SAXS profiles for SI/S02 (50/50) with DOP (ϕ_p = 0.85) near the first-order maximum with temperatures through the order–disorder transition temperature. (b) The reciprocal intensity I_m^{-1} at $q = q_{md} = 2\pi/D_S$, D or D_S, and χ_{eff} as a function of $1/T$ for the same system as in part a.

mination of T_b is aimed to provide a very rough estimate of T_b for the melt systems without DOP. Equation 11 together with $\chi = A + B/T$ in Table III of ref 3 or eq 15 should be used for more quantitative determination of T_b from T_b'.

Table II summarizes ϕ_p used and T_b' determined for the SI and the binary mixtures of SI/HS and their corresponding T_b. Figure 6a shows the typical change of the SAXS profile for a particular mixture of SI/S02 (50/50) in DOP with ϕ_p = 0.85 with temperature below and above the ODT. Here the temperature change of the first-order maximum only was highlighted through the ODT, as only the first-order maximum exists in the disordered state. The temperature dependence of the SAXS profiles at $T \leq 140$ °C is quite different from that at $T \geq 160$ °C. In the lower temperature region, the SAXS maximum decreases in intensity and shifts toward larger q with increasing temperature. This fact and the fact that there exist the higher order maxima (the third-order peak at $q_m/q_{m1} = \sqrt{7}$) up to 130 °C suggest that the mixture is in the ordered state at $T \lesssim 140$ °C and that the change of the SAXS profiles with T is due to that of the segregation power.[14-16] At a temperature slightly higher than 140 °C, the peak scattering vector q_{md} for the first-order SAXS maximum does not shift, but the peak scattered intensity I_m drops with increasing temperature. This fact and the fact that the SAXS profile does not show the higher order maxima indicate that the mixture is in the disordered state at $T \gtrsim 160$ °C.

Figure 6b shows the inverse of the SAXS scattered intensity at $q = q_{md}$ (I_m^{-1}) and the wavelength of the dominant mode of the composition fluctuations of PS and PI segments, D ($=2\pi/q_{m1}$) or D_S ($=2\pi/q_{md}$), as a function of $1/T$. In the disordered state I_m^{-1} decreases approximately linearly with $1/T$, and D_S is independent of $1/T$, as Leibler's Landau-type mean-field theory predicts.[17] The deviations from the linear dependence of I_m^{-1} with T^{-1} and the increase of D with T^{-1}, upon further increase of T^{-1}, are believed to reflect an onset of the ordering and microdomain formation, as discussed in an earlier paper.[12] In this way, the ODT temperature T_b' was determined. All the mixtures SI/HS studied in this work showed the ODT over a relatively narrow temperature range, in comparison with the systems reported by Bates and his co-workers[18,19] for which the ODT cannot be unequivocally determined from the plots of D^{-1} or D_S^{-1} vs T^{-1} and I_m^{-1} vs T^{-1} only. Surprisingly D or D_S was found to show no remarkable change with temperature above and below the ODT.[18,19] This difference in the ODT behavior is not well understood at present and deserves future study. A small curvature in the plot of I_m^{-1} vs T^{-1} at $T > T_b'$ may be due to the finite size effect as elaborated by Frederickson and Helfand for pure A–B type diblock copolymers.[20] $\chi_{eff}(T)$ shown in Figure 6b was determined by the method as fully discussed previously,[3] in the context of the mean-field theory.[17,26]

Figure 7 shows the ODT temperature T_b' as a function of ϕ_{DOP} (for the DOP solution of SI) or T_b as a function of ϕ_{HS} (for the SI/HS mixtures) for various HS with different M_{HS}. The solvent DOP is seen to be most effective in lowering ODT. T_b decreases with increasing ϕ_{HS} for the lower molecular weight HS (e.g., SI/S01 and SI/S02). T_b does not change much with increasing ϕ_{HS} for the higher molecular weight HS (e.g., SI/S04, SI/S10, and SI/S17). T_b for SI/S17 first decreases with ϕ_{HS} and then increases with a further increase of ϕ_{HS}. The above tendency is in good agreement with that predicted by Noolandi et al.[21,22]

3. Temperature Dependence of D in the Ordered State. In this section, we analyzed the wavelength, D, of the dominant mode of the composition fluctuations, as determined from the first-order SAXS maximum in the ordered state

$$D = 2\pi/q_{m1} \quad (1)$$

as a function of T, ϕ_{HS}, M_{HS}, and ϕ_p.

Figure 8 shows a double-logarithmic plot of the temperature dependence of D for SI and SI/S02 in bulk (a) and in DOP (b). The labels L, C, and S attached in each curve on $D(T)$ designate hereafter the lamellar, cylindrical, and spherical microdomain morphology, respectively. The following trends are clearly observed: (i) The values D

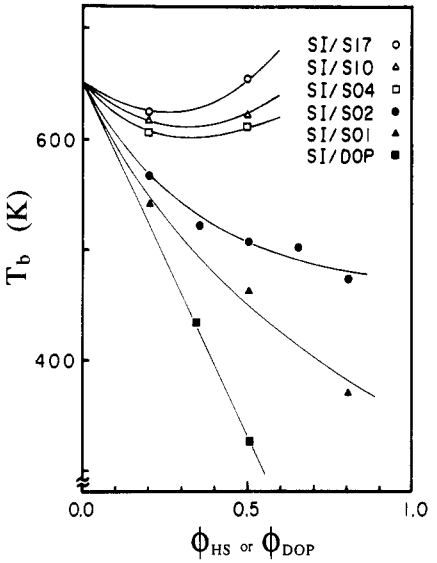

Figure 7. Order–disorder transition temperature T_b'(K) for SI/DOP and T_b(K) for SI/HS mixtures with various homopolymer molecular weights M_{HS} as a function of the volume fraction of HS (ϕ_{HS}) or DOP (ϕ_{DOP}). T_b's for SI/HS in bulk were converted from those for SI/HS with DOP (see text).

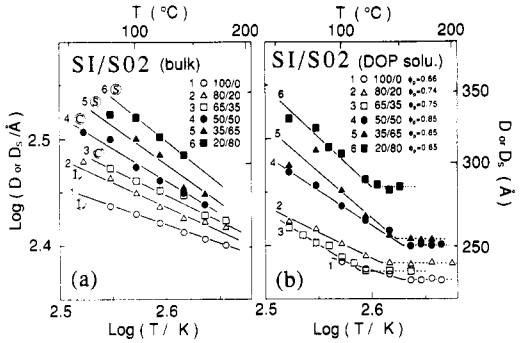

Figure 8. Change of the wavelength of the dominant mode of the composition fluctuations $D = 2\pi/q_{m1}$ in the ordered state (solid lines) or D_S in the disordered state (broken lines) with temperatures for SI and SI/S02 in bulk (a) and in DOP (b). ϕ_p is the total volume fraction of the polymers in SI/S02/DOP systems.

generally decrease with T in the ordered state (solid curves) but remain unchanged in the disordered state (broken lines). (ii) The larger the value ϕ_{HS} ($\simeq W_{HS}$), the larger the value D for both the ordered and disordered states, as discussed intensively in previous companion papers.[1,2] (iii) The larger the value ϕ_{HS}, the larger the temperature dependence of D. The pure block copolymer shows approximately

$$D \sim T^{-1/3} \tag{2}$$

confirming previous experimental reports.[16,23] (iv) An addition of the neutral solvent DOP decreases D, due to the decreasing segregation power between PS and PI segments, as will be discussed in full detail in section IV (cf. parts a and b in Figure 8). The results shown in Figure 8 suggest that

$$D = D(T;\phi_{HS},\phi_p) \sim (1/T)^n \tag{3}$$

and

$$n = n(\phi_{HS}) \geq 1/3 \tag{4}$$

where the limiting value $^1/_3$ is obtained for $\phi_{HS} = 0$. It should be noted that ϕ_p affects the prefactor of $(1/T)^n$ but not the exponent n.

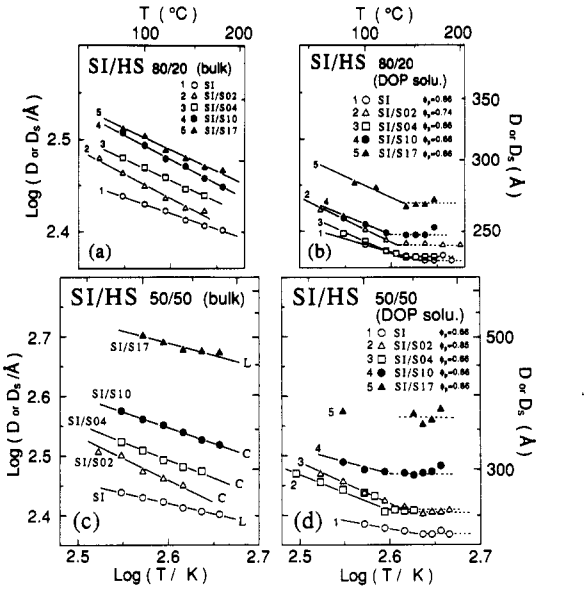

Figure 9. Change of the wavelength of the dominant mode of the composition fluctuations $D = 2\pi/q_{m1}$ in the ordered state (solid lines) or D_S in the disordered state (broken lines) with temperatures for SI and SI/HS with a given composition of 80/20 in bulk (a) and in DOP (b) and for SI and SI/HS with a given composition of 50/50 in bulk (c) and in DOP (d). ϕ_p has the same meaning as in Figure 8.

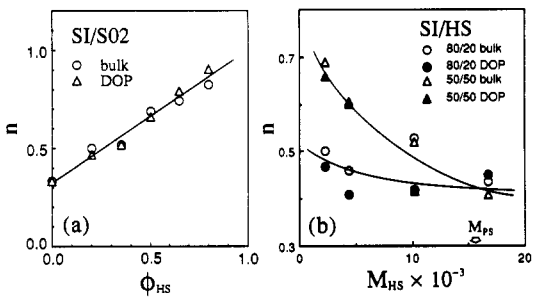

Figure 10. Exponent n in $D \sim T^{-n}$ as a function of ϕ_{HS} (a) and M_{HS} (b). M_{PS} denotes the molecular weight of the PS block chain in the SI block copolymer.

Figure 9 shows the temperature dependence of D for SI/HS (80/20) in bulk (a) and in DOP (b) and for SI/HS (50/50) in bulk (c) and in DOP (d). In addition to the trends i–iv found in Figure 8, D is found to also be a function of M_{HS}; i.e.

$$D = D(T;\phi_{HS},M_{HS},\phi_p) \tag{5}$$

At a given temperature and ϕ_p, D increases with M_{HS}. Moreover, as M_{HS} increases, the temperature dependence, as characterized by n, decreases. Thus, eq 4 is generalized to

$$n = n(\phi_{HS},M_{HS}) \tag{6}$$

Figure 10 summarizes how the slope n, i.e., the temperature dependence of D, depends on ϕ_{HS} (a) and M_{HS} (b) for the mixtures in both bulk and DOP. First, it is found that n is independent of the amount of DOP, within experimental accuracy. This finding is consistent with our earlier finding that D for pure block copolymer is *qualitatively* scaled with χ_{eff}[16]

$$D \sim \chi_{eff}^{1/3} \sim (\chi\phi_p)^{1/3} \sim (\phi_p/T)^{1/3} \tag{7}$$

where the relation of $\chi \sim 1/T$ is assumed. If a corresponding qualitative equation for the binary systems SI/

HS is given by

$$D \sim \chi_{eff}^{n} \sim (\phi_p/T)^n \quad (8)$$

then n becomes independent of ϕ_p as shown in Figure 10, and ϕ_p affects the prefactor of T^{-n}. More *quantitative* scaling of D with χ or χ_{eff} will be given in the next section.

For SI/S02 it is found that

$$n = 0.66\phi_{HS} + 0.33 \quad (9)$$

i.e., the larger the HS content, the larger the temperature dependence of D (see Figure 10a). This trend is seen also for other mixtures (SI/S04 and SI/S10), except for the mixture SI/S17, for which n tends to decrease with increasing ϕ_{HS}, as shown in Figure 10b. Figure 10b shows how the value n, i.e., the temperature dependence of D for the SI/HS mixtures, depends on M_{HS} for a given ϕ_{HS}. It is interesting to note that the coefficient $(\partial n/\partial\phi_{HS})_{M_{HS}}$ tends to change with M_{HS}

$$\left(\frac{\partial n}{\partial \phi_{HS}}\right)_{M_{HS}} \begin{cases} >0 & \text{if } M_{HS} < M_{PS} \quad (10a) \\ \lesssim 0 & \text{otherwise} \quad (10b) \end{cases}$$

IV. Interpretations of $D(T;\phi_{HS},M_{HS},\phi_p)$ or $n = n(\phi_{HS},M_{HS})$

The effect of ϕ_p on n was given in section III-3. Let us now try to give qualitative interpretations to the effects of M_{HS} and ϕ_{HS} on n, i.e., on the temperature dependence of D. This is very much related to the solubilization behavior of HS in the PS microdomains, as discussed previously,[1,2] and its change with segregation power between PS and PI segments invoked by the temperature change, as sketched in Figure 11.

Figure 11 sketches the change of the domain size associated with raising the temperature T from T_0 to T_1 for a pure A–B diblock copolymer (parts a and b), for mixtures of A–B and A homopolymer with relatively small molecular weight M_{HA} so that A tends to be *uniformly solubilized* or to swell uniformly the A microdomains (parts c and d for *uniform swelling*), and for those with relatively large M_{HA} so that A tends to be *locally solubilized* in the middle of the domains or to swell locally the A microdomains (parts e and f for the *localized swelling*).

For the pure block copolymer, the equilibrium domain size is determined by a balance between the entropies, which are associated with *chain conformation* ΔS_{conf} (and hence with the chain stretching) and the placement of the chemical junctions at the interfaces ΔS_p, and the A–B contact energy ΔE at the interface, which is associated with the segregation power.[13-16] By raising temperature from T_0 to T_1, the segregation power decreases, resulting in the entropies outweighing the energetics. Therefore, the chains try to gain more ΔS_{conf} and ΔS_p by invoking the reductions of the domain sizes D from D_{0A}, D_{0B}, and D_0 to D_{1A}, D_{1B}, and D_1, respectively. Needless to say that the reductions of D relax the chain stretching (and hence increase ΔS_{conf}) and increase the average distance a between the chemical junctions from a_0 to a_1 (and hence increase ΔS_p), in order to satisfy the incompressibility requirement. The decreases of D invoke a penalty of increasing ΔE as the interfacial area per unit volume (Σ) increases. However, this penalty is compensated by the increased entropies, ΔS_{conf} and ΔS_p. Thus, the domain size decreases with increasing temperature.

The relatively low molecular weight homopolymers A swell the A microdomain more or less uniformly,[1,2] which increases the thickness of the A microdomain D_A from D_{0A} to D_{0AH} and the distance a from a_0 to a_{0H} and decreases the thickness of the B domain D_B from D_{0B} to D_{0BH} (cf. parts a and c of Figure 11). The decrease of D_B is outweighed by the increase of D_A, giving rise to a net increase of D from D_0 to D_{0H}. The swelling of the A domain involves a further stretching of the A block chains, compared with those in pure block copolymer, and hence the loss of ΔS_{conf} for the A block chain. However, this cost in the free energy is outweighed by the increase of the combinatorial entropy, ΔS_{comb}, in the A domain and by the increase of ΔS_p, both stabilizing the uniform solubilization.

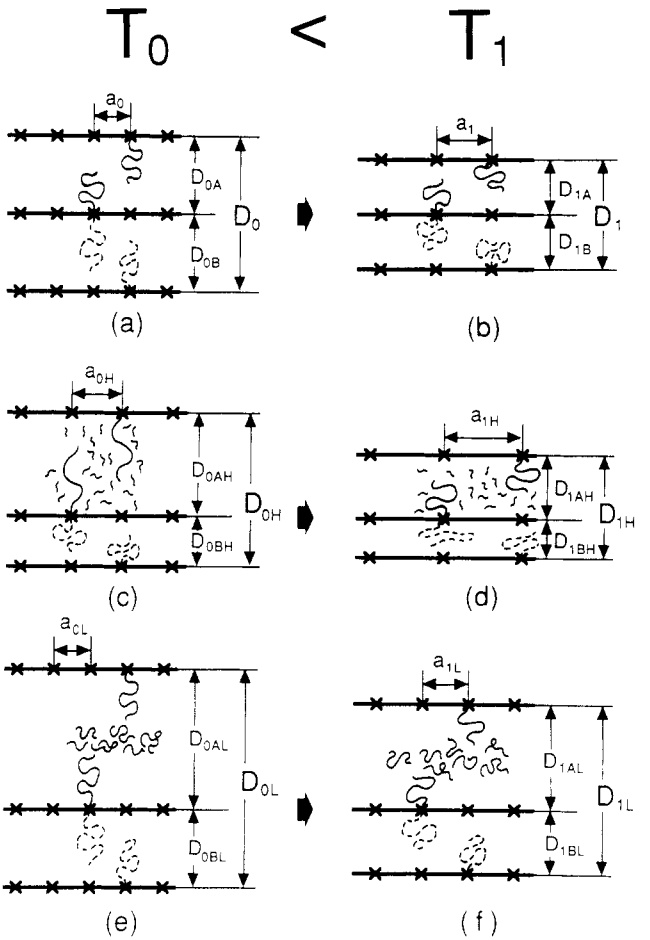

Figure 11. Sketches show the change of the domain size with temperature for pure A–B block copolymer (parts a and b), mixtures of A–B block copolymers and A homopolymers with a relative small molecular weight M_{HA} (parts c and d for the uniform solubilization), and the mixtures of A–B block copolymer and A with relatively large M_{HA} (parts e and f for the localized solubilization). The left and right halves of the sketches correspond to those at lower (T_0) and higher temperature (T_1), respectively.

When the temperature is raised from T_0 to T_1, the domain shrinks longitudinally from D_{0AH}, D_{0BH}, and D_{0H} to D_{1AH}, D_{1BH}, and D_{1H}, respectively, but expands laterally from a_{0H} to a_{1H}, for the same reason as discussed above for the case of the pure block copolymer. The lateral expansion relaxes the stretching of the A block chains and hence the A homopolymer chains as well, thus increasing ΔS_{conf}. It also increases ΔS_p. These entropy gains well compensate the energetic penalty due to the increasing ΔE. ΔS_{comb} remains unchanged, as the total volume of the A microdomain is fixed. These entropy gains by the lateral expansion in the mixtures are much greater than those in the pure block copolymer giving rise to a greater lateral expansion with temperature and hence a greater n. It should be noted that the homopolymers uniformly solubilized also are stretched normal to the interface as they are in the same field of the block chains.[24] Thus the relaxation of the chain stretching for the A block chain is expected to cause the relaxation of the chain stretching for the A homopolymer chains.

As M_{HA} increases, the gain of ΔS_{comb} due to the uniform swelling of the homopolymers A becomes increasingly small. It eventually becomes smaller than the loss of ΔS_{conf} invoked by the swelling, which results in the destabilization of the uniform swelling and promotes the localized solubilization, as shown in parts e and f of Figure 11. In this limit, the *localized solubilization* becomes stable as it involves relaxation of the stretched block chains A and hence increasing ΔS_{conf}, and this increase of ΔS_{conf} outweighs the cost of decreasing ΔS_{comb} invoked by the localized solubilization.[25] The localized solubilization involves only the longitudinal swelling, hence increasing D_A from D_{0A} to D_{0AL}, but essentially no changes in a and D_B. Hence, for a given ϕ_{HA} and at a given T, $D_{0L} > D_{0H}$, hence accounting for the dependence of D on M_{HA}.[2]

When the segregation power is lowered by raising the temperature from T_0 to T_1 for the systems with the *localized swelling*, the entropy gains in ΔS_{conf} and ΔS_p drive the lateral expansion from a_{0L} to a_{1L} and the longitudinal contraction from D_{0AL}, D_{0BL}, and D_{0L} to D_{1AL}, D_{1BL}, and D_{1L}, respectively, for the same reason as discussed in the changes of a to b and of c to d in Figure 11. However, the lateral expansion is expected to be less and hence n is smaller for the locally swollen systems than for the uniformly swollen systems, as the gain of ΔS_{conf} is much less for the former than for the latter. In other words, this is because at T_0 the block chains in the former have more relaxed conformations than those in the latter. Thus, as M_{HA} increases, n becomes small, because A homopolymers tend to be solubilized locally to a greater extent. For the large M_{HA}, the greater the value of ϕ_{HA}, the more likely A homopolymers tend to be solubilized locally, hence giving rise to a smaller value of n, which may account for the striking phenomenon as given by eq 10b.

V. Scaling Behavior of D with χ or χ_{eff}

In the previous section, D was studied as a function of T for various values of M_{HS}, ϕ_{HS}, and ϕ_p. Here we investigate D as a function of a parameter related to the segregation power; i.e., χ_{eff}/χ_{ODT} or $\epsilon_T = |\chi_{eff} - \chi_{ODT}|/\chi_{ODT}$ in the presence of DOP or χ/χ_{ODT} or $\epsilon_T = |\chi - \chi_{ODT}|/\chi_{ODT}$ in bulk. χ_{ODT} is the χ parameter at the ODT. Note that $\chi/\chi_{ODT} \sim \chi N$ for pure block copolymers with a given total degree of polymerization N and a volume fraction of one type of block chain f, as $\chi_{ODT} \sim 1/N$. This expression is approximate because of the finite size effect.[20] For this analysis we utilize the data on the temperature dependence of $\chi = \chi(T;M_{HS},\phi_{HS})$ or $\chi_{eff} = \chi_{eff}(T;\phi_p,M_{HS},\phi_{HS})$ previously estimated for the same set of polymers SI/HS from the SAXS analysis in the disordered state (see Tables II and III of ref 3).

Figure 12 shows a reduced plot for SI and SI/S02 systems where the Bragg spacing D for the ordered microdomains is reduced by the wavelength D_S of the dominant mode of the fluctuations in the disordered state. The reduced spacing D/D_S was double-logarithmically plotted against the reduced interaction parameter χ_{eff}/χ_{ODT} for the systems with DOP (open symbols) or χ/χ_{ODT} for the systems without DOP (filled symbols). It should be noted that χ values for bulk systems were estimated from χ_{eff} values for the corresponding systems with DOP by assuming that

$$\chi_{eff} = \chi\phi_p = (A + B/T)\phi_p \qquad (11)$$

The assumption that underlies eq 11 was fully discussed previously.[3]

Figure 12 clarifies the following points: (i) D increases with increasing segregation power χ_{eff}/χ_{ODT} or χ/χ_{ODT},

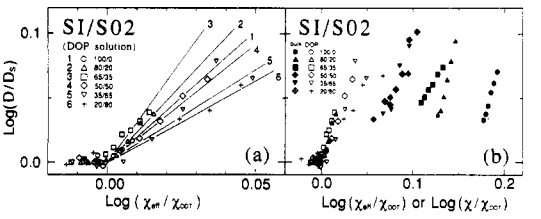

Figure 12. Reduced double-logarithmic plots of D/D_S vs χ_{eff}/χ_{ODT} for the systems with DOP (a) (open symbols) or χ/χ_{ODT} for those without DOP (b) (filled symbols) for SI/S02 mixtures with various W_{HS}. The plot assumes $\chi_{eff} = \chi\phi_p$. D and D_S are the wavelength of the dominant mode of the composition fluctuations in the ordered and disordered state, respectively, and χ_{ODT} is the Flory interaction parameter (χ or χ_{eff}) at the order–disorder transition. Note that the portion of the plots in part b with small values of χ_{eff}/χ_{ODT} ($-0.02 \le \log(\chi_{eff}/\chi_{ODT}) \le 0.05$) was expanded in part a.

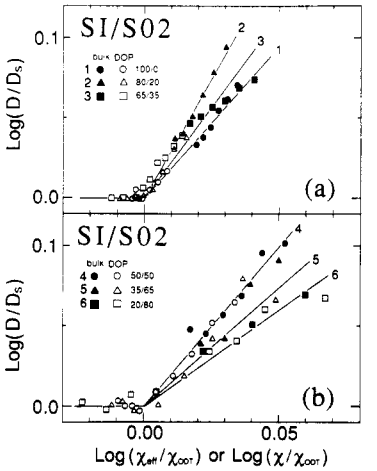

Figure 13. Reduced double-logarithmic plots of D/D_S vs χ_{eff}/χ_{ODT} for the systems with DOP (open symbols) or χ/χ_{ODT} for those without DOP (filled symbols) for SI/S02 mixtures with various W_{HS}. The plot assumes $\chi_{eff} = \chi\phi_p^k$.

but (ii) the rate of increase, depends on W_{HS} (part a). (iii) For any given compositions of SI/HS, the values D/D_S measured as a function of χ_{eff}/χ_{ODT} for the systems with DOP cannot be continuously connected with those measured as a function of χ/χ_{ODT} without DOP (part b). Point iii showing the discontinuity of the data on D/D_S obtained with and without DOP may reflect a problem using eq 11 for the concentration (ϕ_p) dependence of χ_{eff}. The same trends as seen in Figure 12 were observed for all other mixtures SI/HS studied in this work.

Instead of using eq 11, we tried the empirical relation

$$\chi_{eff} = \chi\phi_p^{\,k} = (A + B/T)\phi_p^{\,k} \qquad (12)$$

where k is an adjustable parameter to ensure the continuity of the data on D/D_S obtained with and without DOP. Figure 13 shows the reduced plots for SI (curve 1) and SI/S02 systems (curves 2–6) obtained by using eq 12 instead of eq 11. As shown in the figure, the data obtained with DOP (open symbols) are smoothly connected with those obtained without DOP (filled symbols) on the reduced plots, although log (D/D_s) still depends weakly on W_{HS}. The same trend was observed for other mixtures SI/HS with different molecular weights of HS. Thus it follows that

$$D/D_S \sim [\chi\phi_p^{\,k}/\chi_{ODT}]^m \qquad (13)$$

where m is zero in the disordered state, irrespective of ϕ_p, ϕ_{HS}, and M_{HS} covered in our experiment but nonzero in the ordered state. The value m in the ordered state depends on ϕ_{HS} and M_{HS}; i.e., $m = m(\phi_{HS},M_{HS})$. Figure

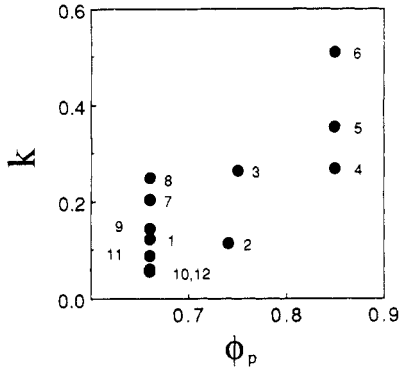

Figure 14. Adjustable parameters k used in obtaining Figure 13 for SI and SI/HS with various M_{HS} and W_{HS} for HS: 1, SI; 2, SI/S02 (80/20); 3, SI/S02 (65/35); 4, SI/S02 (50/50); 5, SI/S02 (35/65); 6, SI/S02 (20/80); 7, SI/S04 (80/20); 8, SI/S04 (50/50); 9, SI/S10 (80/20); 10, SI/S10 (50/50); 11, SI/S17 (80/20); 12, SI/S17 (50/50).

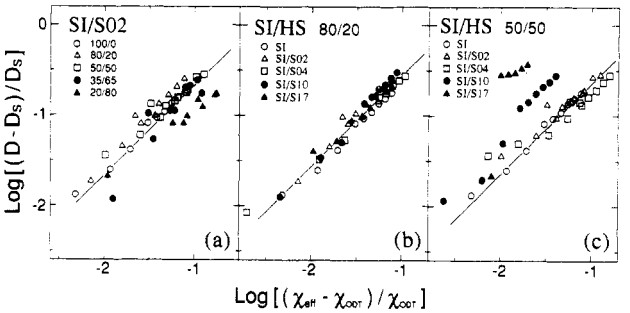

Figure 15. Reduced plots on log $[(D - D_S)/D_S]$ vs log $[(\chi_{eff} - \chi_{ODT})/\chi_{ODT}]$ in the ordered state for (a) SI/S02 mixtures with various W_{HS} and for SI/HS with (b) 80/20 and (c) 50/50 compositions but with various M_{HS}. Note that the plots include the data obtained with and without DOP.

14 shows the values k for various mixtures SI/HS at the three total polymer concentrations ϕ_p's. At a given ϕ_p, the value k tends to increase with increasing W_{HS} for SI/S02 and SI/S04 but with decreasing W_{HS} for SI/S17. The values k exist in the range between 0.1 and 0.5.

After trials and errors we found that the universal relationship of

$$\log\left[\frac{D - D_S}{D_S}\right] = a \log\left[\frac{\chi_{eff} - \chi_{ODT}}{\chi_{ODT}}\right] + b \qquad (14)$$

with $a = 1.006$ and $b = 0.388$ independent of ϕ_p, M_{HS}, and ϕ_{HS} was obtained for the ordered state by assuming that

$$\chi_{eff} = A + B\phi_p^{2/3}/T \qquad (15)$$

where A and B are the constants that determine the temperature dependence of χ for PS and PI segments in bulk; i.e., $\chi = A + B/T$ (see Table III of ref 3). Figure 15 demonstrates the universality of the relationship given by eq 14 for (a) SI and SI/S02 with various W_{HS}, (b) SI and SI/HS with various M_{HS} but a fixed composition of 80/20, and (c) the same as b except for a different composition of 50/50. The plots include the data obtained with and without DOP. Somewhat greater deviations of the data points for SI/S10 and SI/S17 in part c, compared with those for other systems, may reflect the difference in the solubilization behavior as discussed in section IV (i.e., localized vs uniform solubilization). The concentration dependence of χ_{eff} in eq 15 should be experimentally checked in future.

VI. Concluding Remark

The ordered structure of the binary mixtures of SI/HS with various homopolymer compositions (ϕ_{HS}) and molecular weights (M_{HS}) was studied as a function of temperature T, up to the order–disorder transition temperature, by the SAXS method. The binary mixtures were studied in bulk or with an addition of a small amount of the neutral solvent DOP. No distinct morphological changes were observed in the SAXS profiles with temperature and the amount of DOP (ϕ_S) for the pure SI and SI/HS mixtures; i.e., either spherical, cylindrical, or lamellar morphology was observed over the temperature range covered in our experiments. The identity period of the microdomain morphology D generally decreases with temperature according to eqs 3 and 6 with n increasing with increasing ϕ_{HS} and decreasing M_{HS} as discussed in section IV. The data on $D = D(T;\phi_{HS},M_{HS},\phi_p)$ were found to give an empirical scaling law as given by eqs 14 and 15.

Acknowledgment. The authors are grateful to Drs. D. J. Meier, M. D. Whitmore, and J. Noolandi for enlightening comments and discussion. This work is partially supported by a Grant-in-Aid for Scientific Research in Priority Areas "New Functionality Materials Design, Preparation and Control" (No. 02205066) from the Ministry of Education, Science and Culture, Japan.

References and Notes

(1) Tanaka, H.; Hasegawa, H.; Hashimoto, T. *Macromolecules* **1991**, *24*, 240.
(2) Hashimoto, T.; Tanaka, H.; Hasegawa, H. *Macromolecules* **1990**, 23, 4378.
(3) Tanaka, H.; Hashimoto, T. *Macromolecules*, in press.
(4) Zin, C. W.; Roe, R. J. *Macromolecules* **1984**, *17*, 183.
(5) Nojima, S.; Roe, R. J. *Macromolecules* **1987**, *20*, 1866.
(6) Owens, J. N.; Gancarz, I. S.; Koberstein, J. T.; Russell, T. P. *Macromolecules* **1989**, *22*, 3388.
(7) Hashimoto, T.; Suehiro, S.; Shibayama, M.; Saijo, K.; Kawai, H. *Polym. J.* **1981**, *13*, 501.
(8) Fujimura, M.; Hashimoto, T.; Kawai, H. *Mem. Fac. Eng., Kyoto Univ.* **1981**, *43*, 224.
(9) Fujimura, M.; Hashimoto, H.; Kurahashi, K.; Hashimoto, T.; Kawai, H. *Macromolecules* **1981**, *14*, 1196.
(10) Sakurai, S.; Okamoto, S.; Kawamura, T.; Hashimoto, T. *J. Appl. Cryst.*, in press.
(11) Hashimoto, T.; Mori, K. *Macromolecules* **1990**, *23*, 5347.
(12) See, for example: Hashimoto, T. In *Thermoplastic Elastomers*; Legge, N. R., Holden, G., Schroeder, H. E., Eds.; Hanser: Munich Vienna, New York, 1987; Chapter 12.3 and references cited therein.
(13) Meier, D. J. *J. Polym. Sci., Part C* **1969**, *26*, 81.
(14) Helfand, E. *Macromolecules* **1975**, *8*, 552. Helfand, E.; Wasserman, Z. R. *Macromolecules* **1976**, *9*, 879; **1978**, *11*, 960.
(15) Meier, D. J. Reference 12, Chapter 11.
(16) Hashimoto, T.; Shibayama, M.; Kawai, H. *Macromolecules* **1983**, *16*, 1093.
(17) Leibler, L. *Macromolecules* **1980**, *13*, 1602.
(18) Bates, F. S.; Rosedale, J. H. Fredrickson, G. H. *J. Chem. Phys.* **1990**, *92*, 6255.
(19) Bates, F. S.; Fredrickson, G. H. *Annu. Rev. Phys. Chem.* **1990**, *41*, 525.
(20) Fredrickson, G. H.; Helfand, E. *J. Chem. Phys.* **1987**, *87*, 697.
(21) Hong, K. M.; Noolandi, J. *Macromolecules* **1983**, *16*, 1083.
(22) Whitmore, M. D.; Noolandi, J. *Macromolecules* **1985**, *18*, 2486.
(23) Hashimoto, T.; Ijichi, Y.; Fetters, L. J. *J. Chem. Phys.* **1988**, *89*, 2463. Ijichi, Y.; Hashimoto, T.; Fetters, L. J. *Macromolecules* **1989**, *22*, 2817.
(24) Hasegawa, H.; Tanaka, H.; Hashimoto, T.; Han, C. C. *J. Appl. Cryst.*, in press.
(25) Meier, D. J., private communication.
(26) Tanaka, H.; Sakurai, S.; Hashimoto, T.; Whitmore, M. D. *Polymer*, in press.

Registry No. SI, 105729-79-1; polystyrene, 9003-53-6.